PROCEEDINGS OF ECOS 2023 - THE 36TH INTERNATIONAL CONFERENCE ON
EFFICIENCY, COST, OPTIMIZATION, SIMULATION AND ENVIRONMENTAL IMPACT OF ENERGY SYSTEMS
25-30 JUNE, 2023, LAS PALMAS DE GRAN CANARIA, SPAIN

Power vs. capacity performances of thermally integrated MH-PCM hydrogen storage solutions: current status and development perspectives

V. K. Krastev[a], L. Bartolucci[b], G. Bella[c], S. Cordiner[b], G. Falcucci[a] and V. Mulone[b]

[a] Enterprise Engineering Dept., University of Rome "Tor Vergata", Rome, Italy, krastev@dii.uniroma2.it
[b] Industrial Engineering Dept., University of Rome "Tor Vergata", Rome, Italy
[c] Engineering Dept., Niccolò Cusano University, Rome, Italy

Abstract:

The present work focuses on two particular performance indicators for hydrogen storage solutions based on the thermal integration of metal hydrides (MH) with phase-change materials (PCMs): i) the (specific) discharge power and ii) the system-level volumetric capacity. The paper first condenses available literature data from modelling and experimental activities, and then analyses a basic numerical benchmark of a low-temperature MH-PCM system.

Findings from the literature review show that, due to the interrelation between efficient thermal management and hydrogen desorption rate, the selected performance indicators are not independent one from another. It is also confirmed that simultaneously achieving high-power (flexibility) and specific capacity (compactness) is a challenging goal for such kind of hydrogen storage systems. The parametric analysis of the numerical benchmark system suggests that, for a given MH operating pressure-temperature envelope, special care should be given in the PCM accurate characterisation and selection, as well as in the quantification of the optimal trade-off between the PCM volume and desorption kinetics performance. Furthermore it is found that the geometrical distribution of the MH and PCM volumes have a larger than expected impact on the specific discharge power.

Keywords:

Hydrogen Storage; Metal Hydrides; Phase Change Materials; Power; Volumetric Capacity.

1. Introduction

In order to attain a net zero-carbon footprint, it is imperative to produce a substantial share of energy from sustainable sources (IPCC, 2022). Hydrogen is currently recognised as an essential element in facilitating the incorporation of large-scale renewable energy sources (Bartolucci et al., 2021). It also has the potential to become a primary energy carrier, being capable of transporting and distributing energy across various sectors and regions while also improving the energy system's resilience by serving as a buffer (Bartolucci et al., 2023; Kovač et al., 2021). To establish a commercially sustainable H2 economy, it is crucial to store, transport, and distribute H2 as needed for power and heat generation in various applications (Abohamzeh et al., 2021a). Recent research published through the H2 Technology Collaboration Program of the International Energy Agency has provided a positive outlook on the future prospects of H2-based energy storage. Several studies have explored the integration of renewable energy systems with H2 storage to achieve net-zero-emission energy systems and sustainable development goals (Petkov & Gabrielli, 2020). The increasing affordability of H2 utilization technologies, such as fuel cells, may replace battery storage through electrolysers/H2 storage due to their higher efficiency, reliability, and performance (Yue et al., 2021). To present, the cost of H2 systems is higher compared to battery systems, but recent research activities on the H2 value chain for various applications are anticipated to make them competitive by 2030 (Abbasi & Abbasi, 2011).

H2 storage techniques can be broadly categorised into two groups: physical storage and material storage. Physical storage relies on the principle of compression and liquefaction. In contrast, material storage encompasses several systems and provides various utilization methods based on service conditions. Currently, the accepted standard for H2 storage is in high-pressure gaseous form, with storage pressures of up to 700 bar in steel or carbon fibre reinforced polymeric vessels (Nazir et al., 2020). Compressed H2 (CH) technology offers the advantage of fast filling and release rates, as well as lower storage costs. However, CH has several well-known limitations, including reduced storage efficiency, limited volumetric storage capacity, and safety concerns. Compressing H2 from typical production conditions (20 bar) up to 700 bar results in a 9-

https://doi.org/10.52202/069564-0197

12% reduction in net energy stored (Nazir et al., 2020). If Type 4 vessels are considered, the effective volumetric storage capacity of CH at 700 bar is approximately 25 kg/m3. For stationary applications, it is preferable to storage pressures as low as 50 bar or less, for a better integration with renewable H2 generation and to operate under safer conditions. However, at 50 bar, the volumetric capacity of CH systems falls below 2 kg/m3, which would require very large vessels for long-term storage (Abohamzeh et al., 2021b; Maestre et al., 2021).

Metal hydrides (MH) are a promising alternative to replace compressed hydrogen (CH) for stationary applications due to their inherently higher volumetric storage capacity and moderate operating pressures and temperatures (Bellosta von Colbe et al., 2019; El Kharbachi et al., 2020). Mg-based and intermetallic hydrides are the focus of recent MH storage technology development (Ben Mâad et al., 2016; El Mghari et al., 2019, 2020; Garrier et al., 2013; Marty et al., 2013; Mellouli et al., 2015). Mg-based hydrides have attractive reversible gravimetric capacities, material safety, and low cost, but their high reaction enthalpy, high equilibrium temperature, and slow kinetics require catalyst particle additions (Pasquini et al., 2022). Intermetallic hydrides of the AB2 or AB5 types are preferred thanks to their ease of activation, good reversibility, and comparatively fast kinetics (Pasquini et al., 2022). Due to the highly exothermic/endothermic hydrogen absorption/desorption reactions, proper active or passive thermal management is necessary for high-power applications involving MH storage systems (Facci et al., 2021; Nguyen & Shabani, 2021). Active thermal control allows for effective performance tuning, but generates energy losses and may add significant mass and volume at system level (Motyka, 2014). Passive thermal control, specifically through the adoption of phase-change materials (PCMs), is a promising solution due to its energy efficiency gains and inherent simplicity (Nguyen & Shabani, 2021).

Darzi et al. (Rabienataj Darzi et al., 2016) examined how hydrogen is charged and discharged into and from a cylindrical metal hydride tank made of LaNi5, while also studying the heat transfer to a surrounding jacket filled with PCM. El Mghari et al. (El Mghari et al., 2020) analysed five different PCMs and emphasised that the ratio of the total heat of diffusion of the PCM to the total heat of reaction of the MH is a significant factor in achieving complete hydrogenation of the tank. Alqahtani et al. (Alqahtani, Mellouli, et al., 2020) used numerical methods to investigate the hydrogenation and dehydrogenation processes of an MH reactor surrounded by PCM. They doubled the number of interfaces between the MH reactor and PCM by encompassing the MH reactor with a cylindrical sandwich bed filled with PCM, resulting in an 81.5% and 73% improvement in the time required for hydrogenation and dehydrogenation processes, respectively, compared to a conventional MH-PCM system that includes only a single PCM tank (Alqahtani et al., 2020b). Ye et al. (Ye et al., 2020, 2021) proposed a novel MH-PCM unit where a PCM layer is sandwiched between two layers of MH, which exhibited average absorption and desorption rates about 4.5 and 2.4 times higher, respectively, than the traditional cylindrical configuration.

Several authors have examined the advantages of increasing the thermal conductivity of PCMs to improve the performance of hydrogen storage. To achieve this goal, various methods have been explored. For example, Nguyen et al. (Nguyen et al., 2022) investigated the application of an organic PCM for the thermal management of MH hydrogen storage and found that the use of embedded copper foam to enhance thermal conductivity is crucial for achieving an adequate power performance. Chibani et al. (Chibani et al., 2022) conducted numerical analysis to examine the impact of incorporating PCM into metal foam on the performance of hydrogen desorption from MH. Lewis and Chippar (Lewis & Chippar, 2021) studied the charging and discharging of hydrogen in a LaNi5-based reactor equipped with PCM and emphasised the influence of metal foam and its morphology on hydrogen storage and thermal performance, which can enhance hydriding/dehydriding reaction rates. Bourzgarrou et al. (Bouzgarrou et al., 2022) demonstrated that a well-designed U-type heat pipes insert in the metal and PCM media can significantly reduce loading time by up to 88%, depending on the melting temperature.

Although the majority of the papers discussed various methods to improve the power and capacity of MH tanks, they usually did not consider the overall H2 storage capacity at the system level, neither the power/capacity ratio. To address this gap, the authors conducted a thorough analysis of the relevant parameters for some of the studies mentioned above, selecting the ones where all the information required was directly or indirectly available. The purpose of this analysis was to illustrate the difficulty of simultaneously achieving a high discharge power/capacity ratio and a high system-level H2 volumetric storage capacity, as depicted in Figure 1. The current paper aims, therefore, in highlighting capacity and power enhancement factors through a representative MH-PCM computational framework, targeting at the optimisation of both performance indicators.

https://doi.org/10.52202/069564-0197

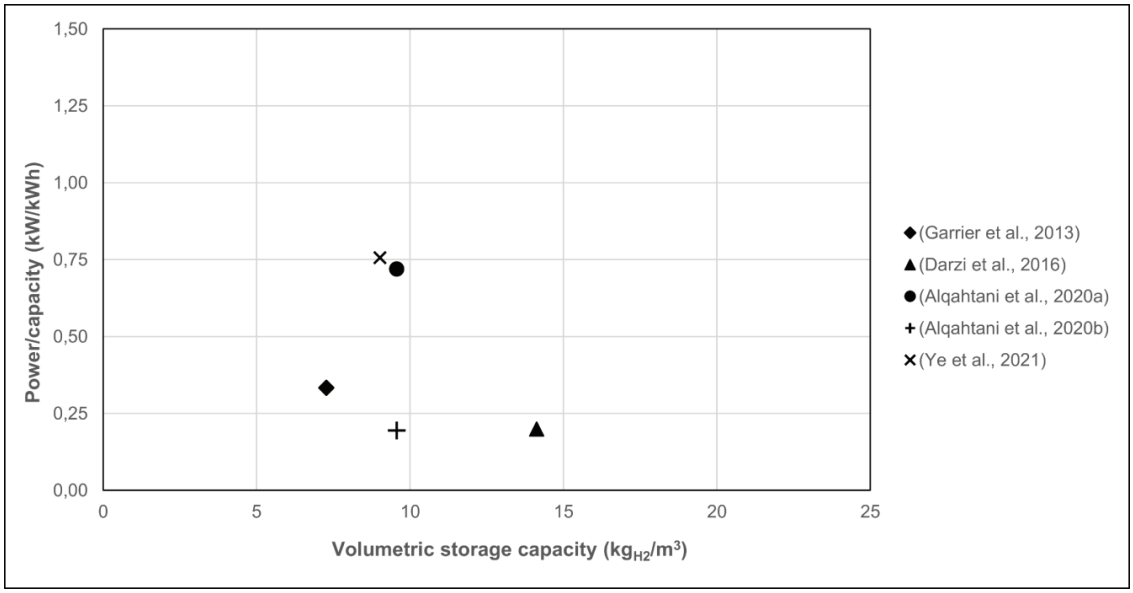

Figure 1. Specific discharge power vs. volumetric storage capacity of MH-PCM systems, literature review.

2. Numerical benchmark

2.1. Problem and setup description

A simple vertically oriented cylindrical MH reactor geometry, surrounded by a PCM-filled jacket, has been taken as a reference for the numerical analysis part of the present work (Figure 2). An analogous MH-PCM system has already been studied during hydrogen filling by two of the authors in a previous publication (Bartolucci & Krastev, 2022) , as well as by other researchers (Alqahtani, Bamasag, et al., 2020b) but none of them focusing on the specific discharge power vs. volumetric capacity performances. The selected MH is a low-temperature intermetallic $LaNi_5$-H_2 system, while the PCM is an inorganic $LiNO_3$-$3H_2O$ salt hydrate. The latter has been recognised in previous research works as one of the best performing PCMs for pairing with low-temperature MHs (Bartolucci & Krastev, 2022; El Mghari et al., 2020). The most relevant MH and PCM properties are listed in Tables 1 and 2. The baseline geometry is exactly equivalent to the one already investigated in (Bartolucci & Krastev, 2022), while it has been subsequently altered to optimise the PCM quantity and to test different slenderness factors H/D, with $D = 2R_i$ (see Table 3).

All the simulations here presented are based on the following main assumptions:

a. the MH-PCM reactors are represented as 2D axisymmetric geometries;
b. the MH bed volume is kept constant for all reactor geometries;
c. the external boundaries of the MH-PCM reactor (except for the hydrogen outlet boundary) are all adiabatic;
d. hydrogen is released from the MH bed at a known and constant pressure (atmospheric pressure);
e. gaseous hydrogen is assumed to follow the ideal gas law;
f. the MH bed is considered as an isotropic porous medium with uniform porosity and permeability;
g. local thermal equilibrium is assumed to hold within the $LaNi_5$-H_2 system;
h. buoyancy is not considered for the heat transfer and melting phenomena within the PCMs;
i. density of the PCM is considered constant and equal to the average between solid and liquid values;
j. other thermophysical properties of PCMs vary with temperature according to the available data, unless differently specified.

The MH-PCM system bed simulation framework has been implemented in ANSYS® Fluent (*ANSYS® Academic Research CFD, Release 2020 R2, Fluent User's Guide*, 2020), combining ad-hoc developed User

https://doi.org/10.52202/069564-0197

Defined Functions (UDFs) for hydrogen desorption with the enthalpy-porosity method (Voller & Prakash, 1987; Voller & Swaminathan, 1991) for phase transition. For a detailed explanation of model equations and of the UDF implementation procedure, the reader is redirected to (Bartolucci & Krastev, 2022). References for the phase transition modelling can be found also in (Krastev & Falcucci, 2021). All the numerical predictions reported here adopt a numerical time step equal to 0.1 s, with a physical simulated time of 10^4 s. All computational grids are made of quad-uniform elements with a 0.5 mm spacing. At the beginning of each simulation, the initial temperature of the system is set to 313 K and the pressure inside the MH tank is set at the equilibrium value for that temperature. Discharge pressure at the tank outlet is 1 bar.

Table 1. Main thermophysical and reaction properties of the $LaNi_5$-H_2 system.

Parameters	*Description*	*Values*
A_d	Plateau coefficient (desorption)	10.57
B_d	Plateau coefficient (desorption)	3704.6 K
C_d	Rate coefficient (desorption)	9.57 s^{-1}
$C_{p,g}$	Specific heat capacity (gas)	14890 J kg^{-1} K^{-1}
$C_{p,s}$	Specific heat capacity (solid)	419 J kg^{-1} K^{-1}
E_d	Activation energy (desorption)	16473 J mol^{-1}
ΔH_R	Enthalpy of reaction	30478 J mol^{-1}
K	Bed permeability	10^{-8} m^2
ε	Bed porosity	0.5
λ_g	Thermal conductivity (gas)	0.1815 W m^{-1} K^{-1}
λ_s	Thermal conductivity (solid)	2 W m^{-1} K^{-1}
μ_g	Dynamic viscosity (gas)	8.4 x 10^{-6} Pa s
ρ_{sat}	Saturated metal density	7259 kg m^3
ρ_{emp}	H_2-free metal density	7164 kg m^3
$w_{\%}$	Gravimetric capacity (bed only)	1.32 %
m_{LaNi5}	Metal mass	~ 0.422 kg
m_{H2}	H2 storage capacity	5.6 g

Table 2. Main thermophysical properties of the $LiNO_3$-H_2O PCM.

Parameters	*Description*	*Values*
$C_{pl,PCM}$	Specific heat capacity (liquid)	2770 J kg^{-1} K^{-1}
$C_{ps,PCM}$	Specific heat capacity (solid)	1730 J kg^{-1} K^{-1}
R_{CP}	Liquid-to-solid C_p ratio	1.6
L_f	Latent heat of fusion	296000 J kg^{-1}
T_m	Melting temperature	303 K
$\lambda_{l,PCM}$	Thermal conductivity (liquid)	0.58 W m^{-1} K^{-1}
$\lambda_{s,PCM}$	Thermal conductivity (solid)	1.32 W m^{-1} K^{-1}
R_λ	Liquid-to-solid λ ratio	0.44
μ_{PCM}	Dynamic viscosity (liquid)	0.0042 Pa s
$\rho_{l,PCM}$	Density (liquid)	1780 kg m^{-3}
$\rho_{s,PCM}$	Density (solid)	2140 kg m^{-3}

Table 3. Dimensional details of the considered jacket-type MH-PCM reactor geometries.

Parameters	*Description*	*Baseline (H/D = 2)*	*Optimised (H/D = 2)*	*Optimised (H/D = 1)*	*Optimised (H/D = 4)*
R_{H2}	H_2 outlet radius	0.5 cm	0.5 cm	0.5 cm	0.5 cm
R_i	Internal radius	2.1 cm	2.1 cm	2.65 cm	1.67 cm
R_e	External radius	3.45 cm	3.2 cm	4.05 cm	2.55 cm
H	Height	8.5 cm	8.5 cm	5.3 cm	13.4 cm
H/D	Slenderness	2	2	1	4
V_{MH}	MH volume (total)	118 cm^3	118 cm^3	118 cm^3	118 cm^3
V_{PCM}	PCM volume	200 cm^3	154 cm^3	154 cm^3	154 cm^3

https://doi.org/10.52202/069564-0197

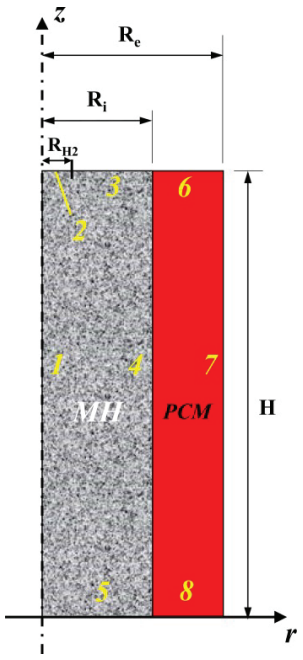

Figure 2. Schematic of the jacket-type MH-PCM cylindrical reactor.

2.2. Results

In this Section, numerical prediction results are shown in terms of the hydrogen discharge dynamics, PCM liquid fraction and temperature evolution in the MH and PCM tanks. Figures 3 and 4 compares the baseline and mass-optimised reactor configurations, where the same slenderness factor (H/D = 2) for the MH container is assumed for both. Note that the PCM mass optimisation was obtained through the following simple relationship between the total enthalpy of reaction of the desorbed H2 mass and the PCM latent heat of fusion:

$$m_{PCM} = \frac{m_{H2} \cdot \Delta H_R}{L_f} . \quad (1)$$

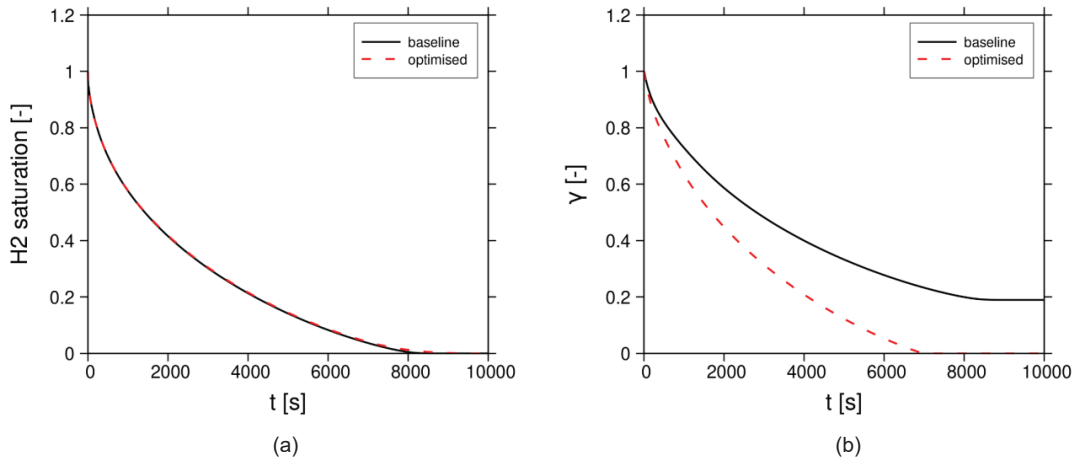

Figure 3. Comparison between the baseline and mass-optimised MH reactor configurations, in terms of a) hydrogen discharge curve and b) PCM liquid fraction over time.

https://doi.org/10.52202/069564-0197

Figure 3a confirms that the baseline and mass-optimised configurations have essentially equivalent H2 discharge performances (both are able to discharge 95% of the absorbed H2 mass within 6800 s, with a 1.2 % deviation among the two), while Figure 3b evidences that around 20% of the PCM latent heat capacity is not exploited in the baseline case. Figures 4a and 4b show that, if the PCM has not undergone full phase transition, the MH-PCM system finds its thermal equilibrium close to the melting temperature. Conversely, if the PCM fully melts before all the H2 mass is completely desorbed, the system's equilibrium temperature is significantly lower (around 294 K vs. around 302 K) and closer to the MH equilibrium temperature at the discharge pressure (around 289 K for this case). The latter is beneficial for a subsequent H2 filling of the MH bed, as it would ensure larger temperature gradients between the MH and PCM containers during the initial phase of the exothermic H2 absorption process.

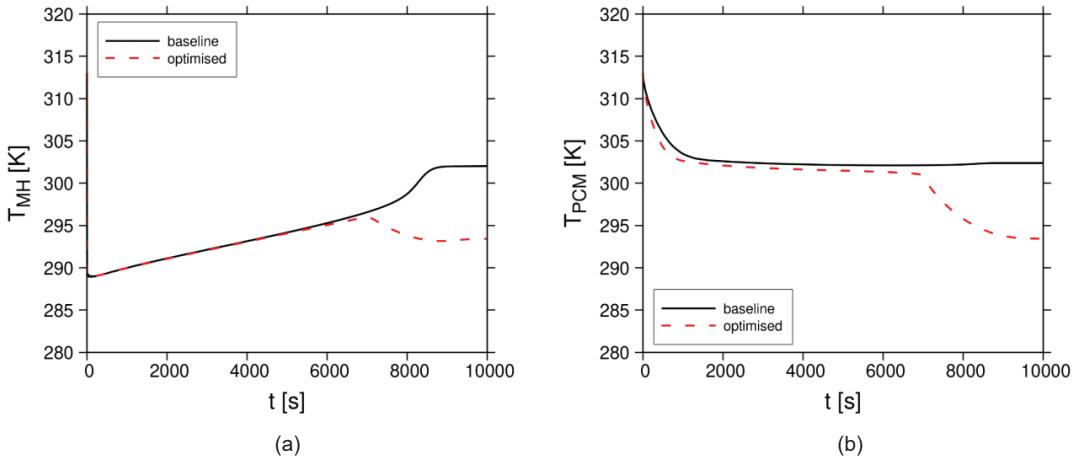

Figure 4. Comparison between the baseline and mass-optimised MH reactor configurations, in terms of a) volume-averaged MH reactor temperature and b) volume-averaged PCM jacket temperature over time.

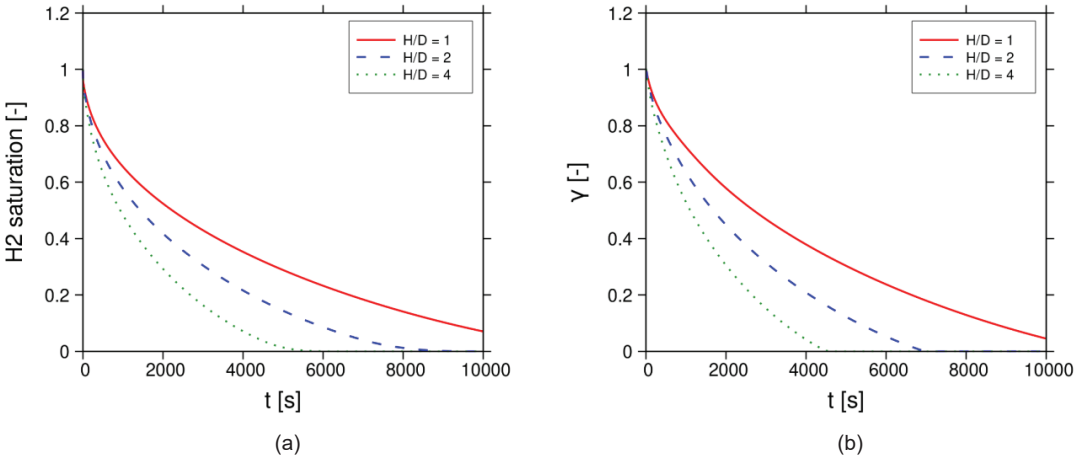

Figure 5. Effects of the slenderness factor H/D on the hydrogen discharge performances: a) hydrogen discharge curve; b) PCM liquid fraction over time.

https://doi.org/10.52202/069564-0197

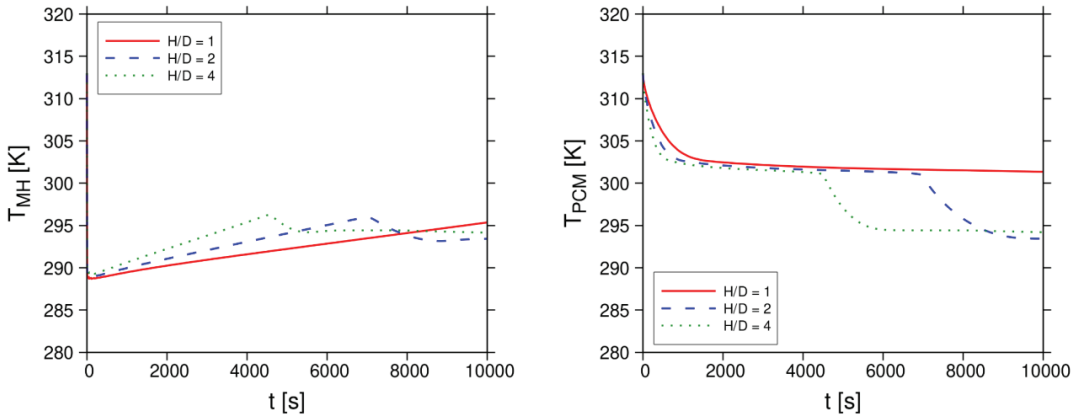

Figure 6. Effects of the slenderness factor H/D on the temperature evolution: a) volume-averaged MH reactor temperature and b) volume-averaged PCM jacket temperature over time.

Figures 5 and 6 allow to evaluate the effect of the slenderness factor H/D on the MH-PCM system discharge dynamics, given the same MH and (optimal) PCM volumes. Raising H/D from 2 to 4 accelerates the hydrogen mass discharge by 37% and thus the average discharge power by 57%. On the opposite, the case with H/D = 1 has a 58% slower discharge dynamics compared to H/D = 2, with the 95% mass discharge actually occurring around 10700 s after the start of the simulation. These differences are most likely to be related to the changes in the radial-wise conductive thermal resistance, as the assumptions listed in Section 2.1 consistently suggests a quasi-1D conductive heat transfer regime in the radial direction, which is also well in line with findings from previous research on cylindrical MH-PCM systems (Bartolucci & Krastev, 2022).

A last series of computations has been performed on the H/D = 2 optimised geometry, changing some of the PCM properties within the simulations. Tests have been made with all constant properties and equal to the solid-liquid average, as well as with reversed Cp and λ liquid-to-solid ratios compared to the actual $LiNO_3$-$3H_2O$ material characteristics. Figure 7 condenses the results obtained, pointing out that: i) using constant and averaged properties introduces acceptable deviations from the actual material behavior (less than 10% deviation on the 95% discharge time); ii) the PCM Cp phase variations have little to no effect on the H2 discharge dynamics; iii) during H2 discharge, the PCM starts to immediately solidify at the PCM-MH heat transfer interface: the solid-phase radial thermal conductivity has, therefore, a dominant effect and when it falls below the MH effective radial conductivity (Reversed R_λ case) it might significantly slow down discharge dynamics.

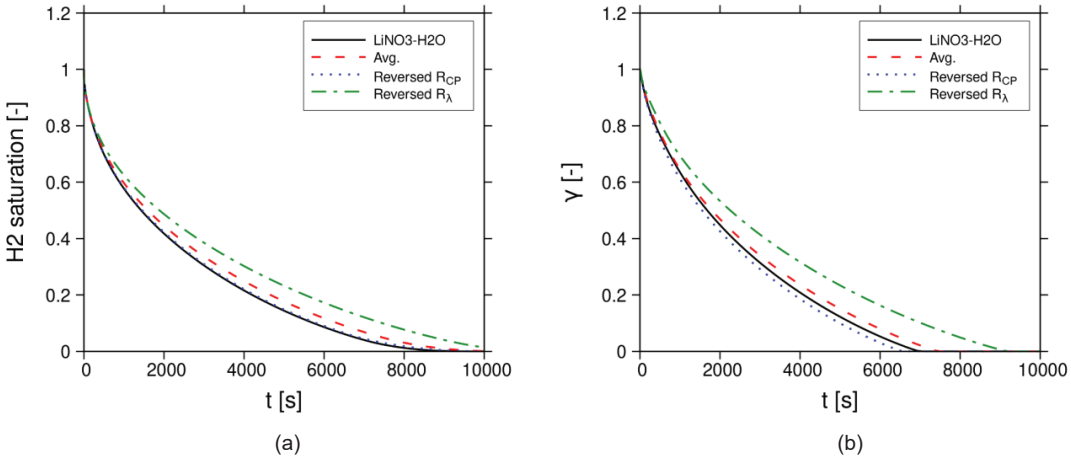

Figure 7. Effects of changes in the PCM properties on the hydrogen discharge performances: a) hydrogen discharge curve; b) PCM liquid fraction over time.

https://doi.org/10.52202/069564-0197

Figure 8 resumes the major findings from the numerical simulations, within the context of the literature review already presented in the Introduction Section. Unsurprisingly, to reach system-level volumetric capacities above 15 kg_{H2}/m^3 it is essential to optimise the minimum required PCM mass and an effective first-level optimization can be made through simple latent heat-based principles. In that regard, selecting PCMs with high densities and latent heat of fusion, such as salt hydrates in the low-temperature PCM range, brings obvious additional benefits.

In terms of specific discharge power, an accurate geometrical optimization of the MH-PCM system, which must take into account the actually dominant heat transfer mechanisms, is crucial. Significant improvements can be potentially achieved even for very simple cylindrical layouts, with no complex conduction-enhancing solutions (e. g. metal fins or foams, blends with graphite fibres or other nano-particles). Still, theoretical and simulation based results has to be verified in realistic engineering environments, taking into account some complex material behaviour that might have been purposely omitted at modelling level: a typical example, related to the findings of the present work, is the well known tendency of salt hydrates to undesired vertical phase separation, which might be difficult to control or minimise in slender vertical containers.

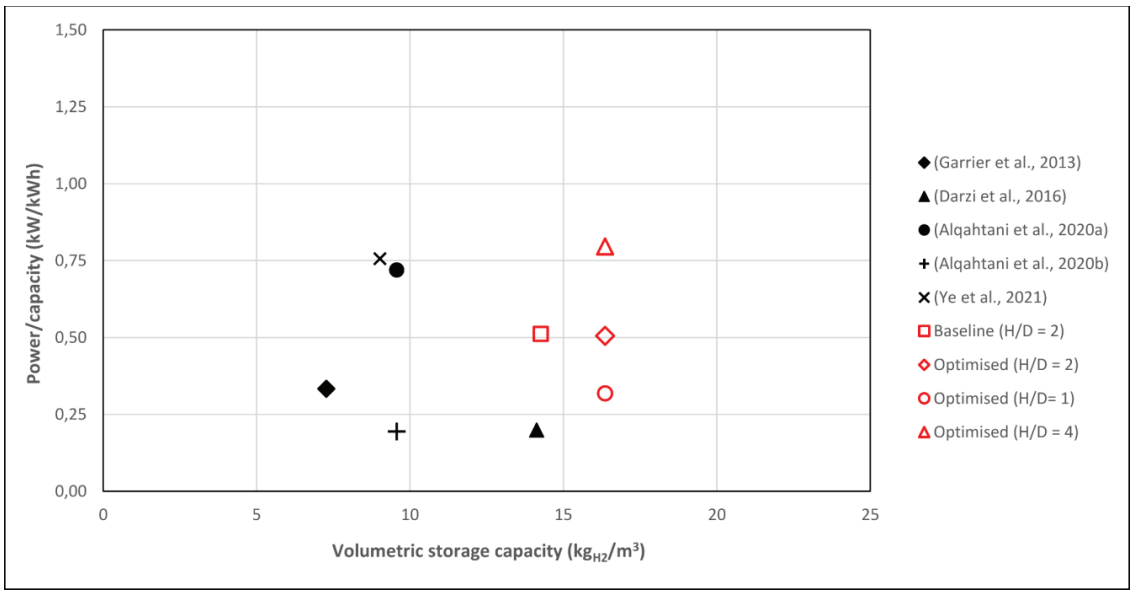

Figure 8. Specific discharge power vs. volumetric storage capacity of MH-PCM systems, literature review (black symbols) and results from the numerical benchmark analysed in the present work (red symbols).

4. Conclusions

From the literature analysis and numerical simulation results shown in this paper, the following conclusions can be drawn regarding MH-PCM system performances during hydrogen discharge:

- although it is often difficult to extract reliable performance indicators from the published works, the previously proposed systems cannot generally simultaneously achieve power/capacity ratios and system-level volumetric storage capacities above 0.75 kW/kWh and 15 kg_{H2}/m^3, respectively;
- the proposed numerical benchmark demonstrates that, in the case of jacket-like cylindrical MH-PCM configurations, these threshold can be exceeded through relatively simple optimization steps, like PCM mass optimization and system shape (slenderness factor H/D) optimization;
- mass optimization of the PCM is essentially linked to the latent heat of fusion, volume optimization comes as a consequence once the PCM density is also considered;

https://doi.org/10.52202/069564-0197

- for vertically-oriented jacket-like systems, higher slenderness factors significantly increase specific discharge power for a given volumetric capacity: is reported that moving from H/D = 1 to H/D = 4 produces a 150% power gain, peaking at a power/capacity ratio of 0.8 kW/kWh;
- the influence of the slenderness factor is explained by the quasi-1D nature of the heat transfer phenomena in this specific discharge case: heat transfer is dominated by conduction in the radial direction and, as such, it is accelerated by lowering the thermal resistance in that direction (smaller radial thicknesses);
- following the previous point, increasing the thermal conductivity in the radial direction both in the MH bed and PCM is also beneficial for a power increase; in that sense, on the PCM side the solid phase thermal conductivity plays the major role during hydrogen discharge (PCM solidification);

Future developments will include a further expanded literature research and the analysis of additional performance influence factors, such as the hydrogen discharge pressure, alternative MH-PCM system geometries, MH pressure-temperature-kinetics envelope.

Acknowledgments

The present research work has received financial support from the Italian Ministry of Universities and Research, Project of National Interest, PRIN 2020BFX8JY - HySuM. V. K. K. acknowledges financial support from the MEGACELL departmental research project, CUP n. E83C22006060005.

References

Abbasi, T., & Abbasi, S. A. (2011). “Renewable” hydrogen: Prospects and challenges. In *Renewable and Sustainable Energy Reviews* (Vol. 15, Issue 6, pp. 3034–3040). https://doi.org/10.1016/j.rser.2011.02.026

Abohamzeh, E., Salehi, F., Sheikholeslami, M., Abbassi, R., & Khan, F. (2021a). Review of hydrogen safety during storage, transmission, and applications processes. *Journal of Loss Prevention in the Process Industries*, *72*. https://doi.org/10.1016/j.jlp.2021.104569

Abohamzeh, E., Salehi, F., Sheikholeslami, M., Abbassi, R., & Khan, F. (2021b). Review of hydrogen safety during storage, transmission, and applications processes. *Journal of Loss Prevention in the Process Industries*, *72*. https://doi.org/10.1016/j.jlp.2021.104569

Alqahtani, T., Bamasag, A., Mellouli, S., Askri, F., & Phelan, P. E. (2020a). Cyclic behaviors of a novel design of a metal hydride reactor encircled by cascaded phase change materials. *International Journal of Hydrogen Energy*, *45*(56), 32285–32297. https://doi.org/10.1016/j.ijhydene.2020.08.280

Alqahtani, T., Bamasag, A., Mellouli, S., Askri, F., & Phelan, P. E. (2020b). Cyclic behaviors of a novel design of a metal hydride reactor encircled by cascaded phase change materials. *International Journal of Hydrogen Energy*, *45*(56), 32285–32297. https://doi.org/10.1016/j.ijhydene.2020.08.280

Alqahtani, T., Mellouli, S., Bamasag, A., Askri, F., & Phelan, P. E. (2020). Thermal performance analysis of a metal hydride reactor encircled by a phase change material sandwich bed. *International Journal of Hydrogen Energy*, *45*(43), 23076–23092. https://doi.org/10.1016/j.ijhydene.2020.06.126

ANSYS® Academic Research CFD, Release 2020 R2, Fluent User’s Guide. (2020). ANSYS Inc.

Bartolucci, L., Cordiner, S., Mulone, V., & Pasquale, S. (2021). Hydrogen based Multi Energy Systems: Assessment of the marginal utility of increasing hydrogen penetration on system performances. *International Journal of Hydrogen Energy*, *46*(78), 38588–38602. https://doi.org/10.1016/j.ijhydene.2021.09.108

Bartolucci, L., Cordiner, S., Mulone, V., Tatangelo, C., Antonelli, M., & Romagnuolo, S. (2023). Multi-hub hydrogen refueling station with on-site and centralized production. *International Journal of Hydrogen Energy*. https://doi.org/10.1016/j.ijhydene.2023.01.094

Bartolucci, L., & Krastev, V. K. (2022). On the Thermal Integration of Metal Hydrides with Phase Change Materials: Numerical Simulation Developments towards Advanced Designs. *SAE Technical Papers*. https://doi.org/10.4271/2022-24-0018

Bellosta von Colbe, J., Ares, J. R., Barale, J., Baricco, M., Buckley, C., Capurso, G., Gallandat, N., Grant, D. M., Guzik, M. N., Jacob, I., Jensen, E. H., Jensen, T., Jepsen, J., Klassen, T., Lototskyy, M. V., Manickam, K., Montone, A., Puszkiel, J., Sartori, S., … Dornheim, M. (2019). Application of hydrides in hydrogen

 https://doi.org/10.52202/069564-0197

storage and compression: Achievements, outlook and perspectives. *International Journal of Hydrogen Energy*, *44*(15), 7780–7808. https://doi.org/10.1016/j.ijhydene.2019.01.104

Ben Mâad, H., Miled, A., Askri, F., & Ben Nasrallah, S. (2016). Numerical simulation of absorption-desorption cyclic processes for metal-hydrogen reactor with heat recovery using phase-change material. *Applied Thermal Engineering*, *96*, 267–276. https://doi.org/10.1016/j.applthermaleng.2015.11.093

Bouzgarrou, F., Mellouli, S., Alqahtani, T., & Algarni, S. (2022). Parametric study of a metal hydride reactor with phase change materials and heat pipes. *International Journal of Energy Research*, *46*(4), 4588–4598. https://doi.org/10.1002/er.7451

Chibani, A., Merouani, S., & Bougriou, C. (2022). The performance of hydrogen desorption from a metal hydride with heat supply by a phase change material incorporated in porous media (metal foam): Heat and mass transfer assessment. *Journal of Energy Storage*, *51*. https://doi.org/10.1016/j.est.2022.104449

El Kharbachi, A., Dematteis, E. M., Shinzato, K., Stevenson, S. C., Bannenberg, L. J., Heere, M., Zlotea, C., Szilágyi, P., Bonnet, J. P., Grochala, W., Gregory, D. H., Ichikawa, T., Baricco, M., & Hauback, B. C. (2020). Metal Hydrides and Related Materials. Energy Carriers for Novel Hydrogen and Electrochemical Storage. *Journal of Physical Chemistry C*, *124*(14), 7599–7607. https://doi.org/10.1021/acs.jpcc.0c01806

El Mghari, H., Huot, J., Tong, L., & Xiao, J. (2020). Selection of phase change materials, metal foams and geometries for improving metal hydride performance. *International Journal of Hydrogen Energy*, *45*(29), 14922–14939. https://doi.org/10.1016/j.ijhydene.2020.03.226

El Mghari, H., Huot, J., & Xiao, J. (2019). Analysis of hydrogen storage performance of metal hydride reactor with phase change materials. *International Journal of Hydrogen Energy*, *44*(54), 28893–28908. https://doi.org/10.1016/j.ijhydene.2019.09.090

Facci, A. L., Lauricella, M., Succi, S., Villani, V., & Falcucci, G. (2021). Optimized modeling and design of a pcm-enhanced h2 storage. *Energies*, *14*(6). https://doi.org/10.3390/en14061554

Garrier, S., Delhomme, B., De Rango, P., Marty, P., Fruchart, D., & Miraglia, S. (2013). A new MgH2 tank concept using a phase-change material to store the heat of reaction. *International Journal of Hydrogen Energy*, *38*(23), 9766–9771. https://doi.org/10.1016/j.ijhydene.2013.05.026

IPCC. (2022). Mitigation Pathways Compatible with 1.5°C in the Context of Sustainable Development. In *Global Warming of 1.5°C* (pp. 93–174). Cambridge University Press. https://doi.org/10.1017/9781009157940.004

Kovač, A., Paranos, M., & Marciuš, D. (2021). Hydrogen in energy transition: A review. *International Journal of Hydrogen Energy*, *46*(16), 10016–10035. https://doi.org/10.1016/j.ijhydene.2020.11.256

Krastev, V. K., & Falcucci, G. (2021). Comparison of enthalpy-porosity and lattice Boltzmann-phase field techniques for the simulation of the heat transfer and melting processes in LHTES devices. *E3S Web of Conferences*, *312*, 01002. https://doi.org/10.1051/e3sconf/202131201002

Lewis, S. D., & Chippar, P. (2021). Analysis of Heat and Mass Transfer During Charging and Discharging in a Metal Hydride - Phase Change Material Reactor. *Journal of Energy Storage*, *33*. https://doi.org/10.1016/j.est.2020.102108

Maestre, V. M., Ortiz, A., & Ortiz, I. (2021). Challenges and prospects of renewable hydrogen-based strategies for full decarbonization of stationary power applications. In *Renewable and Sustainable Energy Reviews* (Vol. 152). Elsevier Ltd. https://doi.org/10.1016/j.rser.2021.111628

Marty, P., De Rango, P., Delhomme, B., & Garrier, S. (2013). Various tools for optimizing large scale magnesium hydride storage. *Journal of Alloys and Compounds*, *580*(SUPPL1). https://doi.org/10.1016/j.jallcom.2013.02.169

Mellouli, S., Ben Khedher, N., Askri, F., Jemni, A., & Ben Nasrallah, S. (2015). Numerical analysis of metal hydride tank with phase change material. *Applied Thermal Engineering*, *90*, 674–682. https://doi.org/10.1016/j.applthermaleng.2015.07.022

Motyka, T. (2014). Hydrogen Storage Engineering Center of Excellence Metal Hydride Final Report. *SRNL-STI-2014-00226*.

Nazir, H., Muthuswamy, N., Louis, C., Jose, S., Prakash, J., Buan, M. E., Flox, C., Chavan, S., Shi, X., Kauranen, P., Kallio, T., Maia, G., Tammeveski, K., Lymperopoulos, N., Carcadea, E., Veziroglu, E., Iranzo, A., & Kannan, A. M. (2020). Is the H2 economy realizable in the foreseeable future? Part II: H2 storage, transportation, and distribution. In *International Journal of Hydrogen Energy* (Vol. 45, Issue 41, pp. 20693–20708). Elsevier Ltd. https://doi.org/10.1016/j.ijhydene.2020.05.241

Nguyen, H. Q., Mourshed, M., Paul, B., & Shabani, B. (2022). An experimental study of employing organic phase change material for thermal management of metal hydride hydrogen storage. *Journal of Energy Storage*, *55*. https://doi.org/10.1016/j.est.2022.105457

Nguyen, H. Q., & Shabani, B. (2021). Review of metal hydride hydrogen storage thermal management for use in the fuel cell systems. In *International Journal of Hydrogen Energy* (Vol. 46, Issue 62, pp. 31699–31726). Elsevier Ltd. https://doi.org/10.1016/j.ijhydene.2021.07.057

Pasquini, L., Sakaki, K., Akiba, E., Allendorf, M. D., Alvares, E., Ares, J. R., Babai, D., Baricco, M., Bellosta Von Colbe, J., Bereznitsky, M., Buckley, C. E., Cho, Y. W., Cuevas, F., De Rango, P., Dematteis, E. M., Denys, R. V., Dornheim, M., Fernández, J. F., Hariyadi, A., … Yartys, V. A. (2022). Magnesium- and intermetallic alloys-based hydrides for energy storage: Modelling, synthesis and properties. In *Progress in Energy* (Vol. 4, Issue 3). Institute of Physics. https://doi.org/10.1088/2516-1083/ac7190

Petkov, I., & Gabrielli, P. (2020). Power-to-hydrogen as seasonal energy storage: an uncertainty analysis for optimal design of low-carbon multi-energy systems. *Applied Energy*, *274*(April), 115197. https://doi.org/10.1016/j.apenergy.2020.115197

Rabienataj Darzi, A. A., Hassanzadeh Afrouzi, H., Moshfegh, A., & Farhadi, M. (2016). Absorption and desorption of hydrogen in long metal hydride tank equipped with phase change material jacket. *International Journal of Hydrogen Energy*, *41*(22), 9595–9610. https://doi.org/10.1016/j.ijhydene.2016.04.051

Voller, V. R., & Prakash, C. (1987). A fixed grid numerical modelling methodology for convection-diffusion mushy region phase-change problems. *Int. J. Heat Mass Transfer*, *30*(8), 1709–1719.

Voller, V. R., & Swaminathan, C. R. (1991). GENERAL SOURCE-BASED METHOD FOR SOLIDIFICATION PHASE CHANGE. *Numerical Heat Transfer, Part B*, *19*, 175–189.

Ye, Y., Ding, J., Wang, W., & Yan, J. (2021). The storage performance of metal hydride hydrogen storage tanks with reaction heat recovery by phase change materials. *Applied Energy*, *299*. https://doi.org/10.1016/j.apenergy.2021.117255

Ye, Y., Lu, J., Ding, J., Wang, W., & Yan, J. (2020). Numerical simulation on the storage performance of a phase change materials based metal hydride hydrogen storage tank. *Applied Energy*, *278*. https://doi.org/10.1016/j.apenergy.2020.115682

Yue, M., Lambert, H., Pahon, E., Roche, R., Jemei, S., & Hissel, D. (2021). Hydrogen energy systems: A critical review of technologies, applications, trends and challenges. In *Renewable and Sustainable Energy Reviews* (Vol. 146). Elsevier Ltd. https://doi.org/10.1016/j.rser.2021.111180

https://doi.org/10.52202/069564-0197